Stability Issues of Low-Energy Intense Beams

K.Y. Ng and A.V. Burov

Fermi National Accelerator Laboratory,[1] *P.O. Box 500, Batavia, IL 60510*

Abstract. Some stability issues of low-energy intense beams are discussed. These include inductor tuners for the cancellation of the longitudinal space-charge induced potential-well distortion and their consequences, transient beamloading and possible feed-forward alleviation, coherent and incoherent transverse tune shifts, as well as the impact of transverse space charge on transverse mode-coupling instability.

I INTRODUCTION

Several relatively low-energy and very high-intensity proton rings, such as the storage rings of the U.S. and European neutron spallation sources, the booster of the Japan Hadron Project, and the low-energy ring of the Fermilab future booster, are under design [1–4]. These rings have circumferences around 150 to 200 m, containing $\sim 1 \times 10^{14}$ protons per cycle. High intensity and low energy imply large space-charge forces in the longitudinal and transverse directions. The longitudinal space-charge force will counteract significantly the rf focusing force giving rise to a large potential-well distortion. To cope with this distortion, one method is to insert inductor tuners to cancel the longitudinal space-charge force. This insertion together with its consequences will be discussed. The intense charge density will also impact large transient beamloading onto the rf cavities. A feed-forward scheme to alleviate the beamloading voltage is addressed. Transversely, the importance of the coherent and incoherent space-charge tune shifts for an intense low-energy beam is reviewed. Finally, the effect of space charge on transverse mode-coupling instability is investigated.

II LONGITUDINAL SPACE CHARGE

Let us take, for example, an older design of the low-energy ring in the Fermilab future booster, which accelerates 2 bunches each containing $N_b = 5.0 \times 10^{13}$ protons from kinetic energy 1.0 GeV to 4.5 GeV at 15 Hz. The ring has a circumference of 180.649 m, rf harmonic $h = 2$, and transition gamma $\gamma_t = 7$. The 95% bunch area is $A = 1.0$ eV-s and 95% normalized emittance $\epsilon_{95} = 200 \times 10^{-6}$ πm. The average current in the ring is $I_{\rm av} = 23.27$ A and the peak current is $I_{\rm pk} = I_{\rm av}/B = 93.06$ A, where $B = 0.25$ is the *bucket bunching factor*. Assuming parabolic distribution, the half bunch length is $\hat{\tau} = 3eN_b/(4I_{\rm pk}) = 64.56$ ns. The half momentum spread is therefore $\hat{\delta} = A/(\pi\hat{\tau}) = 3.322 \times 10^{-3}$. The average betatron function and average dispersion of the ring are, respectively, $\langle\beta\rangle = 25$ m and $\langle D\rangle = 1.8$ m. Thus, the average beam radius is about $a = [\epsilon_{95}\langle\beta\rangle/(\gamma\beta) + (\langle D\rangle\hat{\delta})^2]^{1/2} = 5.29$ cm. A beam

[1] Operated by the Universities Research Association, Inc., under contract with the U.S. Department of Energy.

pipe of radius $b \sim 8$ cm will be recommended. We can therefore estimate the longitudinal space-charge impedance of the ring [5]:

$$\left.\frac{Z_0^{\parallel}}{n}\right|_{\rm spch} = -j\frac{Z_0}{2\gamma^2\beta}\left(1+2\ln\frac{b}{a}\right) = 92.11\ \Omega\ , \tag{2.1}$$

where $\gamma = 2.0658$ and $\beta = 0.8750$ are the Lorentz factors at injection while $Z_0 \approx 377\ \Omega$ is the free-space impedance. This is not bad for microwave instability, because the operation is below transition and the Keil-Schnell stability limit is

$$\left|\frac{Z_0^{\parallel}}{n}\right| \le F_{\parallel}\frac{E_0|\eta|}{e\beta^2 I_{\rm pk}}\left[\frac{\Delta E}{E_0}\right]^2_{\rm FWHM} = 78.86\ \Omega\ , \tag{2.2}$$

where E_0 is the total energy of the synchronous particle and $F_{\parallel} = 1.047$ is the form factor for a bunch with parabolic momentum distribution.

A Potential-Well Distortion and Inductor Insertion

Ignoring coupling impedances, for a bunch with the half length and half momentum spread specified above, the rf bucket holding the bunch must have a synchrotron tune ν_s and a rf voltage $V_{\rm rf}$,

$$\nu_s = \frac{|\eta|\hat{\delta}}{\omega_0\hat{\tau}} = 1.207\times10^{-3}\ , \qquad V_{\rm rf}\cos\phi_s = \frac{2\pi\beta^2E_0\nu_s^2}{|\eta|h} = 31.73\ {\rm kV}\ , \tag{2.3}$$

where $\omega_0/(2\pi) = 1.452$ MHz is the revolution frequency and ϕ_s is the synchronous angle. Therefore, a particle with time advance τ ahead the synchronous particle will see the relative rf voltage

$$V_{\rm rf}[\sin(\phi_s - h\omega_0\tau) - \sin\phi_s] \approx -V_{\rm rf}\cos\phi_s\left[\frac{3\pi B}{2}\right]\frac{\tau}{\hat{\tau}} = -37.38\frac{\tau}{\hat{\tau}}\ {\rm kV}\ , \tag{2.4}$$

where the rf sine wave has been linearized. However, the intense beam creates on the particle a strong repulsive longitudinal electric field

$$E_z^{\rm spch} = -\frac{eZ_0}{4\pi\gamma^2\beta^2c}\left[1+2\ln\frac{b}{a}\right]\frac{d\lambda}{d\tau}\ , \tag{2.5}$$

where c is the velocity of light. Assuming the linear parabolic bunch distribution $\lambda(\tau) = 3eN_b/(4\hat{\tau})(1-\tau^2/\hat{\tau}^2)$, the space-charge voltage seen per turn is

$$V_{\rm spch} = E_z^{\rm spch}C = \frac{3\pi I_b}{(\omega_0\hat{\tau})^2}\left|\frac{Z_0^{\parallel}}{n}\right|_{\rm spch}\frac{\tau}{\hat{\tau}} = +29.11\frac{\tau}{\hat{\tau}}\ {\rm kV}\ , \tag{2.6}$$

where C is the circumference of the accelerator ring. As a result, to maintain the bunch shape, such as the length and momentum spread, the rf voltage required must be increased to $V_{\rm rf} = (37.38+29.11)31.73/37.38 = 56.43$ kV.

If we do not want such a large rf voltage brought about by the space-charge force, we need to cancel the space charge by, for example, inductor insertion. Two such experiments have been performed lately.

1. Fermilab-Los Alamos Collaboration

In 1997, the Los Alamos PSR was running at 797 MeV with an intensity of 3×10^{13} protons in the beam. The space-charge force was intense and an rf voltage of 10 kV was required to bunch the beam so that the injection-extraction gap could be kept clean. Two ferrite tuners designed to cancel $\frac{2}{3}$ of the space charge were built, each ~ 76 cm long consisting of 30 Toshiba M_4C_{21A} cores (12.7 cm I.D., 20.3 cm O.D., and 2.54 cm thick). The relative magnetic permeability is $\mu = 50$ to 70 over a modest temperature range. These properties remain approximately constant up to 30 MHz, after which μ rolls off. A solenoid was wound outside so that relative magnetic permeability could be decreased through perpendicular biasing.

The experiment was performed in August of 1997 [6]. First, bunch lengthening was observed when the ferrite was biased (Fig. 1 left) as was expected with the decrease of the inductance. Second, the rf voltage required for bunching was reduced by about $\frac{1}{3}$, indicating that the space-charge force had been cancelled partially by the inductance of the ferrite (Fig. 1 right). Third, the injection-extraction gap during the experiment was probably the cleanest ever observed.

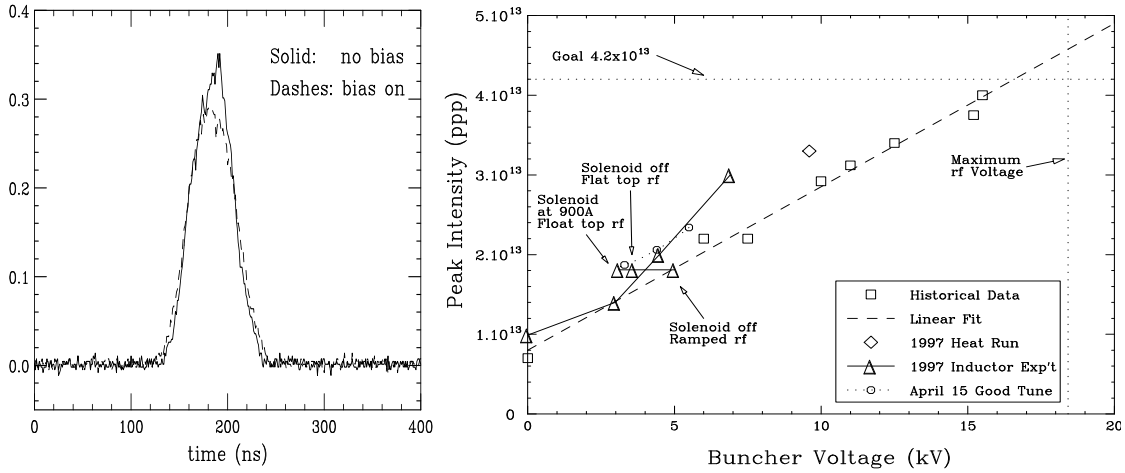

FIGURE 1. Left: PSR beam bunch shapes with unbiased (solid) and biased (dashes) ferrite compensation. Right: Stability threshold versus rf bunching voltage. Results of this experiment are depicted by triangles. (Reproduced from Ref. 6).

2. KEK experiment

A similar experiment started at the KEK PS Main Ring in 1997, but with a much lower intensity of 2 to 9×10^{11} protons per bunch [7]. The beam kinetic energy was 500 MeV with a space-charge impedance $Z_0^{\parallel}/n = -j310\ \Omega$. Instead of ferrite, a Met-Glass-like material called Finemet was used. The inductor tuner consisted of 12 Finemet cores (14.0 cm I.D., 34.0 cm O.D., and 2.54 cm thick), without current biasing. The control of the relative permeability was achieved by installing copper short bars across the Finemet cavities. The coherent frequency of the quadrupole synchrotron oscillation was measured as a function of bunch intensity. As shown in Fig. 2, with the inductor tuner on, the coherent frequency was less dependent on intensity, indicating that the space-charge force had been partially cancelled.

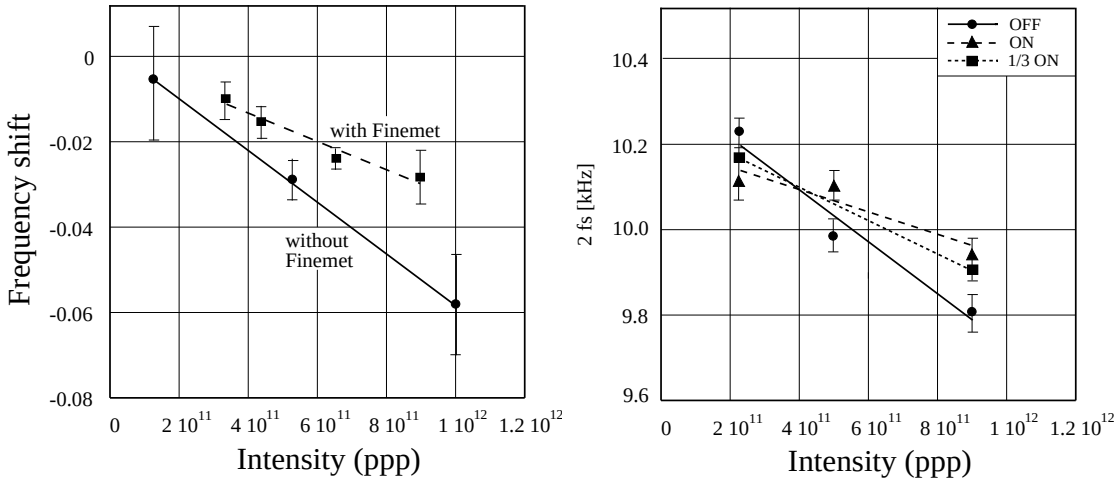

FIGURE 2. Left: Measured frequency shifts of the quadrupole oscillations versus beam intensity at KEK with and without Finemet. Right: New KEK results of quadrupole oscillation frequency versus beam intensity with Finemet tuners on, $\frac{1}{3}$ on, and off. (Reproduced from Ref. 7).

B Power Loss to Ferrite or Finemet

To incorporate loss, the relative permeability can be made complex: $\mu \to \mu' - j\mu''$. The impedance of the ferrite is therefore

$$\frac{Z_0^{\|}}{n} = j(\mu' - j\mu'')\omega_0 L \ , \tag{2.7}$$

where L denotes the inductance of the ferrite or Finemet required to compensate for the space charge of the bunch. It is clear that μ' and μ'' must be frequency-dependent. Their general behaviors are shown in the left plot of Fig. 3. For the Toshiba M_4C_{21A} ferrite, μ' is roughly constant at $\mu'_L \sim 50$ at low frequencies and starts to roll off around $\omega_r/(2\pi) \sim 30$ MHz, while μ'', being nearly zero at low frequencies, reaches a maximum μ''_R near $\omega_r/(2\pi)$. For the Finemet this roll-off frequency can be at very much lower frequency, around 1 to 10 MHz. Thus the power loss to the inductor tuners from the beam may become very large and may not be ignored. First, the energy lost by the beam has to be compensated by the rf system. Second, the ferrite or Finemet can become too warm. Third, a large $\mathcal{R}e\, Z_0^{\|}$ of the inductor can lead to microwave instability. In fact, such an instability had been already observed in the 1997 Los Alamos experiment, and this instability has been much more serious at the present moment when the PSR beam intensity has been upgraded to $\sim 5.0 \times 10^{13}$ protons as indicated in right plot of Fig. 3.

Essentially, the loss is the overlap integral of the bunch spectrum and $\mathcal{R}e\, Z_0^{\|}$ of the inductor tuners. To compute this, an impedance model for the inductor tuners is necessary. The simplest 2-parameter model consists of an *ideal* inductance L and an *ideal* resistor R in parallel, which gives

$$Z_0^{\|}(\omega) = j\omega L \frac{1 - j\omega/\omega_r}{1 + \omega^2/\omega_r^2} \propto j\omega(\mu' - j\mu'') \ , \qquad \omega_r = \frac{R}{L} \ . \tag{2.8}$$

The corresponding longitudinal wake potential is $W(t) = R\,[\,\delta(t) - \omega_r e^{-\omega_r t}\,]$. A 3-parameter model is the broadband parallel-RLC resonance:

$$Z_0^{\parallel}(\omega) = \frac{R}{1 + jQ\left(\dfrac{\omega}{\omega_r} - \dfrac{\omega_r}{\omega}\right)}\,, \tag{2.9}$$

where ω_r is roughly where μ'' peaks. The other two parameters R and Q can be obtained in terms of μ'_L, the value of μ' at low frequencies, and μ''_R, the value of μ'' at resonant frequency $\omega_r/(2\pi)$. From Eq. (2.7), we obtain

$$\left|\frac{Z_0^{\parallel}}{n}\right|_{\rm ind} = \mu'_L \omega_0 L \qquad \text{and} \qquad \mathcal{R}e\, Z_0^{\parallel}(\omega_r) = \mu''_R \omega_r L\,, \tag{2.10}$$

where $|Z_0^{\parallel}/n|_{\rm ind}$ is the inductor impedance per harmonic. From Eq (2.9), we obtain

$$\left|\frac{Z_0^{\parallel}}{n}\right|_{\rm ind} = \frac{\omega_0 R}{Q\omega_r} \qquad \text{and} \qquad \mathcal{R}e\, Z_0^{\parallel}(\omega_r) = R\,. \tag{2.11}$$

Thus, we can solve for $\mu''_R = Q\mu'_L$. Note that Q here is the quality factor describing the μ'' peak. It relates the values of μ' and μ'' at *different* frequencies, and is not the usual industrial-quoted Q which relates them at the *same* frequency.

The energy the particle lost to the inductor in one passage can now be computed:

$$\mathcal{E} = \frac{3e^2 N_b \tau}{2\omega_0 \hat{\tau}^3}\left|\frac{Z_{\parallel}}{n}\right|_{\rm ind} + \frac{3e^2 N_b}{2Q\omega_0\omega_r \hat{\tau}^3}\left|\frac{Z_{\parallel}}{n}\right|_{\rm ind}\,, \tag{2.12}$$

where a parabolic bunch distribution has been used and $Q\omega_r\hat{\tau} \gg 1$ has been assumed. The first term is the linear force from the inductive impedance $Z_{\parallel}/n|_{\rm ind} = j\omega_0 L$, which is supposed to cancel the space-charge force, leaving behind the second

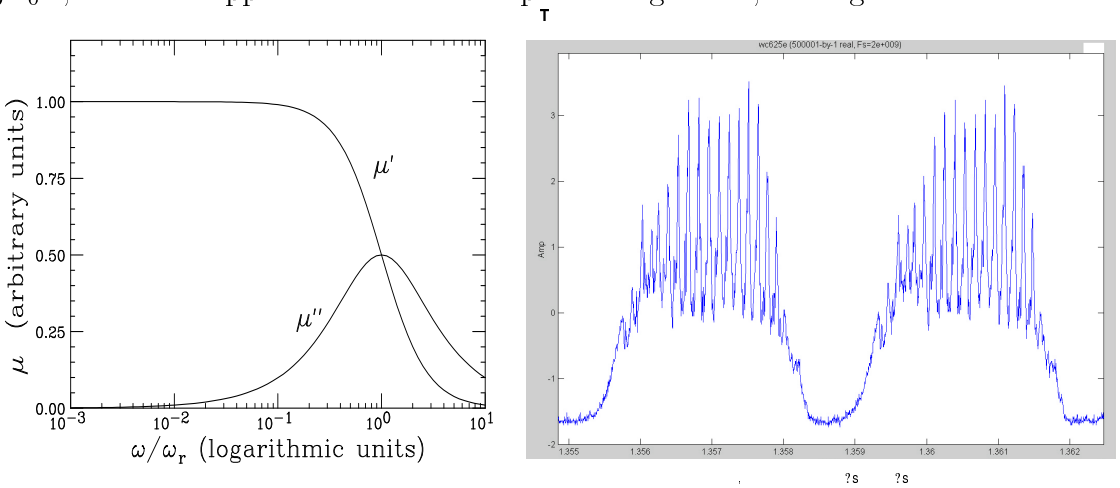

FIGURE 3. Left: A typical plot of μ' and μ'' as functions of frequency. Right: Longitudinal microwave instability observed in a chopped coasting beam (for 2 turns) at the Los Alamos PSR. The collective frequency of the instability is around 75 MHz. Because of the increase in momentum spread, some protons will be rotated into the injection-extraction gap through synchrotron oscillations. They trap electrons leading to transverse e-p instability.

term, which is the actual energy lost to the insertion. For the RL model under the same assumption, exactly the same result is obtained if we make the substitution $Q = 1$. Thus for n_b bunches the total power lost to the insertion becomes

$$P = \frac{3e^2 n_b N_b^2}{4\pi Q \omega_r \hat{\tau}^3} \left| \frac{Z_\parallel}{n} \right|_{\rm ind} . \tag{2.13}$$

Numerical evaluations in various rings are listed in Table 1, where a full compensation by ferrite or Finemet and $Q = 1$ in the resonance model of Eq. (2.9) are assumed. Although the energy lost by a particle per turn is in general small, the total power lost to the ferrite can become big when the bunch is short and intense. For example, in the new design of the Fermilab future booster, the loss of 361 kW to the ferrite is large, although it is tolerable with water cooling. However, for some future machines with, for example, bunch length shortened by another factor of 10, this power loss will increase by a factor of 1000, and will certainly become intolerable.

TABLE 1. Energy loss per turn and total power loss to ferrite or Finemet at various rings.

	KEK	PSR	Fermilab Future Booster	
			Old design	New design
N_b	$2-9\times10^{11}$	$3.0-5.0\times10^{13}$	5.0×10^{13}	2.5×10^{13}
n_b	1	1	2	4
$\hat{\tau}$ (ns)	44	100	64.56	28.25
$Z_0^\parallel/n\|_{\rm spch}$ (Ω)	310	200	100	100
Ferrite: $f_r = 30$ MHz				
$\mathcal{E}$ (keV)	0.221−0.992	0.183−0.344	2.60	13.6
P (kW)	0.0047−0.096	2.45−6.82	60.4	361
Finemet: $f_r = 5$ MHz				
$\mathcal{E}$ (keV)	1.32−5.95	1.10−1.83	15.6	81.4
P (kW)	0.0028−0.058	14.7−40.9	362	2160

C Perpendicular Bias to Saturation

The loss to the ferrite is mainly hysteresis effect. In the hysteresis B-H plot on the left side of Fig. 4, the loss due to one complete oscillation of the ac magnetic field H_1 produced by the beam is proportional to the enclosed area marked 1. If the ferrite is biased with a dc magnetic field H at Point 2, the hysteresis area will be smaller and so is the loss. If we bias at Point 3 at saturation, there will not be any hysteresis loop due to the ac magnetic field H_1 and therefore all hysteresis loss will be eliminated. This strong dc bias field H_c will leave the magnetization $\vec{M}$ precessing around it, and the only loss will be due to the spin wave inside the ferrite, which is small. The price we need to pay here is a much lower relative permeability, which is equal to the slope the line joining the origin to Point 3. Thus more ferrite cores will be needed to compensate for the same amount of space charge. Such a bias scheme can be achieved by encircling the ferrite rings with a solenoid, where the dc biasing field H_c is along the beam direction and is perpendicular to the ac

field H_1 carried by the beam. In fact, such a solenoid is always needed so that the relative permeability can be suppressed as the space charge decreases while the beam particles are ramped. A schematic picture of the precessing magnetization is shown in the right plot of Fig. 4.

Without the hysteresis loss, there will not be any broadband loss peak. There is still a resonance at the much higher gyromagnetic circular frequency of $\omega_c = \gamma_g H_c$, where $\gamma_g = 2\pi \times 2.80$ MHz/Oersted is the gyromagnetic ratio. By choosing the suitable biasing field H_c, this resonant frequency can be made at least 10 times higher than ω_r where the broadband loss peaks but is absent now in the presence of the saturated biasing. This resonance peak is very much narrower and the quality factor is $Q \lesssim 10$. Thus, we can see from Eq. (2.13) that the power loss can be reduced by at least a factor of ~ 100.

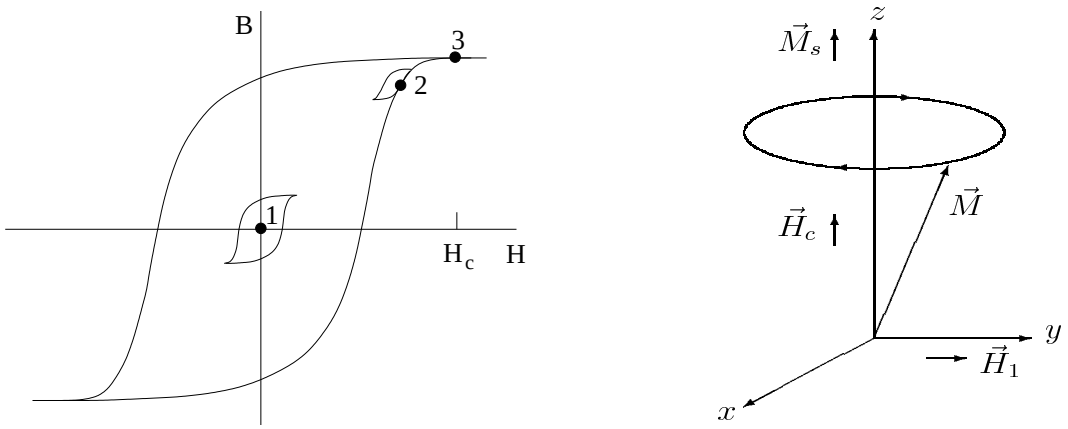

FIGURE 4. Left: Hysteresis B-H plot. At zero bias, the loss is proportional to the enclosed area marked 1. With dc bias field at Point 2, the hysteresis loss will be smaller. At saturated bias at Point 3, all hysteresis loss will be eliminated. Right: System with saturated perpendicular bias H_c in the z-direction. With the application of the ac field $\vec{H}_1$ in the y-direction, the magnetization $\vec{M}$ acquires an ac component in the x-y plane precessing about the z-axis.

D Microwave Instability

Actual area of beam stability in the complex $Z_0^{\parallel}$-plane (or the traditional U'-V' plane) is somewhat different from the commonly quoted Keil-Schnell estimation. In Fig. 5, the heart-shape solid curve, denoted by 1, is the threshold curve for parabolic distribution in momentum spread, where the momentum gradient is discontinuous at the ends of the spread. Instability develops and a smooth momentum gradient will result at the ends of the spread, changing the threshold curve to that of a distribution represented by 2, for example, $\frac{15}{16}(1-\delta^2/\hat{\delta}^2)$. Further smoothing of the momentum gradient at the ends of the spread to a Gaussian distribution will change the threshold curve to 3. On the other hand, the commonly known Keil-Schnell threshold is denoted by the circle of unit radius in dots. This is the reason why in many low-energy machines the Keil-Schnell limit has been significantly overcome by a factor of about 5 to 10. In this case, the space charge is almost the only source of the impedance, the real part of the impedance can be typically orders

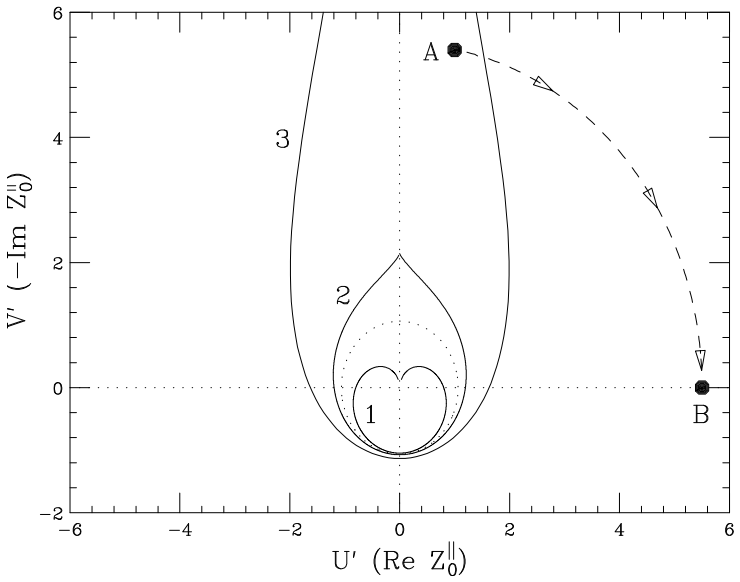

FIGURE 5. Microwave instability threshold curves in the complex $Z_0^{\parallel}$ (or U'-V') plane, for (1) parabolic momentum distribution, (2) distribution with a continuous momentum gradient, and (3) Gaussian momentum distribution. The commonly quoted Keil-Schnell threshold criterion is denoted by the circle in dots. An intense space-charge beam has impedance denoted by Point A outside the Keil-Schnell circle. A ferrite tuner compensating the space charge completely will have a resistive impedance roughly at Point B and is therefore unstable.

of magnitude smaller. As an example, if the impedance of the Los Alamos PSR is at Point A, the beam is within the microwave stable region if the momentum spread is Gaussian like, although it exceeds the Keil-Schnell limit. Now, if we compensate the space-charge potential-well distortion by the ferrite inductance, the ferrite required will have an inductive impedance at low frequency equal to the negative value of the space charge impedance at A, for example, about -5.5 units according to Fig. 5. However, the ferrite also has a resistive impedance or $\mathcal{R}e\, Z_0^{\parallel}$. Although $\mathcal{R}e\, Z_0^{\parallel}/n$ is negligible at low frequencies, it reaches a peak value near $\omega_r/(2\pi)$ (about 50 to 80 MHz for the Toshiba M_4C_{21A}) with the peak value the same order of magnitude as the low-frequency $\mathcal{I}m\, Z_0^{\parallel}$. Actually, according to the RLC model discussed above, we get

$$\frac{\mathcal{R}e\, Z_0^{\parallel}/n|_{\rm pk}}{\mathcal{I}m\, Z_0^{\parallel}/n|_{\omega\to 0}} \approx \frac{Q^2+Q+1}{Q+2} = \left\{ \begin{array}{ll} Q & \text{if } Q \gg 1 \\ 1 & \text{if } Q \sim 1 \\ \frac{1}{2} & \text{if } Q \ll 1 \end{array} \right\} \geq \frac{1}{2}\,. \tag{2.14}$$

The RL model gives the same impedance ratio of $\frac{1}{2}$ as the low-Q case of Eq.(2.14). Thus the ferrite will contribute a resistive impedance denoted roughly by Point B (~ 5.5 units) when $Q \sim 1$ or at least one half of it when $Q \ll 1$. This resistive impedance of the ferrite will certainly exceed the threshold curve and we believe that the longitudinal instability observed at the Los Alamos PSR is a result of this consideration. It follows from here that such low-frequency compensation of an intense space-charge induced potential-well distortion will definitely result in the microwave instability at high frequencies, $\omega \simeq \omega_r$. In other words, the strong

space-charge potential-well distortion can only be compensated by the ferrite or Finemet inductance to a small extent to ensure that the resistive part of the ferrite or Finemet is kept below the microwave instability threshold.

For the transverse bias of the ferrite to saturation discussed in the previous section, although the power dissipation in the ferrite can be reduced to a large extent, the sharp gyromagnetic resonance resulting at higher frequency can become more susceptible to microwave instability, unless the gyromagnetic resonance is very much narrower the width of the bunch spectrum.

E Transient Beamloading

The intense proton beam will excite modes of oscillation in the rf cavities when passing through them. This is called transient beamloading. For the new design of the Fermilab low-energy booster ring, a total rf voltage of ~ 185 kV is required. Since the rf frequency is low, about 7.5 MHz, one needs to split the rf system into 10 cavities, each with $V_{\rm rf} = 18.5$ kV. Each cavity is loaded with 30 cm of ferrite cores ($\mu' = 21$) with inner/outer radii 20/35 cm. This gives an inductance of $L \sim 0.61$ μH and capacitance $C \sim 820$ μF. Then for a point bunch containing $N_b = 2.5 \times 10^{13}$ protons, the transient beam loading voltage is

$$V_{t0} = \frac{eN_b}{C} = 5.4 \text{ kV} , \tag{2.15}$$

which is an appreciable fraction of the $V_{\rm rf} = 18.5$ kV supplied by the klystron. For a longer bunch, the transient beamloading will be less. In fact, this is just the wake potential seen by a particle at time τ ahead the bunch center due to the wake of a cavity gap, or for a Gaussian bunch,

$$V_t(\tau) = e\int_\tau^\infty d\tau' \lambda(\tau') W(\tau' - \tau) = -\frac{eN_b\omega_r R_\parallel}{2Q\cos\phi_0} \mathcal{R}e\, e^{j\phi_0 - \tau^2/(2\sigma_\tau^2)} w\left[\frac{\sigma\tau\omega_r e^{j\phi_0}}{\sqrt{2}} - \frac{j\tau}{\sqrt{2}\sigma_\tau}\right] , \tag{2.16}$$

where $\omega_r/(2\pi)$ is the resonant frequency, $R_\parallel$ the shunt impedance, and Q the quality factor of the cavity mode excited, $\phi_0 = \sin^{-1}\frac{1}{2Q}$, and w is the complex error function. It is easy to show that as the bunch length $\sigma_\tau \to 0$, $V_t(\tau)$ approaches the point-bunch limit V_{t0} in Eq. (2.15).

Let us understand how the transient beamloading originates. As a bunch of protons passes through the cavity gap, a negative charge equal to that carried by the bunch will be left by the image current at the upstream end of the cavity gap. Since the negative image current will resume from the downstream end of the cavity gap following the bunch, an equal amount of positive charge will accumulate there. Thus, a voltage will be created at the gap opposing the beam current and this is the transient beamloading voltage as illustrated in Fig. 6 left. Griffin [8] suggested to use a feed-forward system, which will monitor the linear charge distribution of the bunch and deliver via a tetrode the same amount of negative charge density to the downstream end of the cavity gap so as to cancel the positive charge there and thus alleviating the transient beamloading, as illustrated in Fig. 6 right.

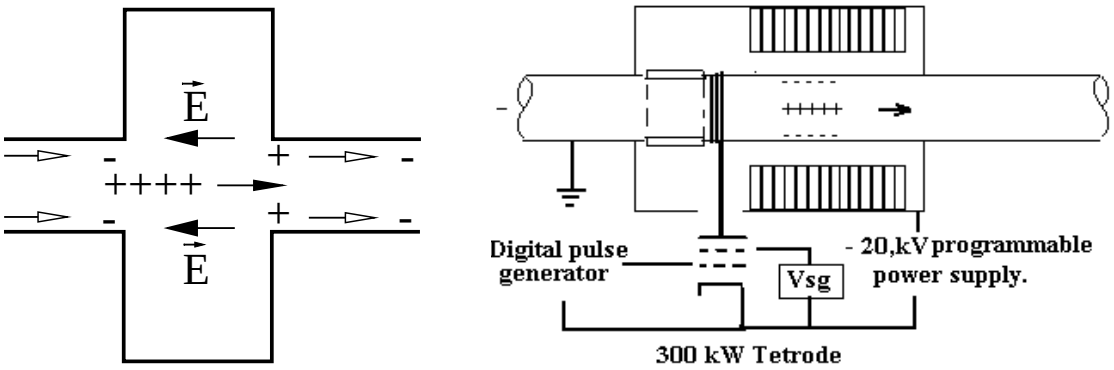

FIGURE 6. Left: As a positively charged bunch passes through a cavity, the image current leaves a negative charge at the upstream end of the cavity gap. As the image current resumes at the downstream side of the cavity, a positive charge is created at the downstream end of the gap because of charge conservation, thus setting up an electric field $\vec{E}$ and therefore the transient beamloading voltage. Right: The bunch density is monitored and a negative charge density is fed-forward through a tetrode to the downstream side of the cavity gap to cancel the positive charge left there, thus eliminating the transient beamloading.

III TRANSVERSE SPACE-CHARGE EFFECTS

A Coherent and Incoherent Tune Shifts

Usually, people say that a large incoherent space-charge tune spread will encompass a lot of parametric resonances and lead to instability. The common rule of thumb is that incoherent self-field tune spread should not exceed ~ 0.40. Both rings of the future Fermilab booster are designed to have normalized 95% emittances equal to 2.0×10^{-4} πm, so that such tune spreads can be below 0.40. However, this self-field tune spread at injection has never been a well-measured beam parameter. It is difficult to measure because low-energy rings are usually ramped very rapidly.

Machida and Ikegami [9] pointed out at the space-charge workshop at Shelter Island that it is the *coherent* rather than the *incoherent* tune shifts that determine the instability of a beam. In fact, this is quite reasonable. When the bunch is oscillating at an integer coherent tune, we have the usual integer resonance. This leads to an instability because all particles are performing betatron oscillations with a tune component that is at an integer. The whole beam will become unstable. On the other hand, if the incoherent tune spread covers an integer resonance, only *a small amount* of particles are hitting the integer resonance; thus the whole beam may not be unstable. The coherent betatron tune is not affected by space charge when the image forces are small. This is because the centroid of the bunch does not see any space-charge force. On the other hand, the coherent quadrupole betatron tune and coherent sextupole betatron tune will be affected by space charge. Therefore, when they hit a resonance, there will be instability. This is demonstrated by the simulation of Machida and Ikegami in Fig. 7. In the simulation, the horizontal coherent quadrupole tune hits the integer of 13 when the beam intensity reaches ~ 15 A. We do see that the horizontal emittance increases rapidly around the beam

intensity of 15 A. The vertical coherent quadrupole tune hits the integer 11 when the beam intensity is raised to around 13 to 15 A. The vertical emittance increases also around those intensities. However, we do not see any growth of emittance when the coherent quadrupole tunes cross half integers.

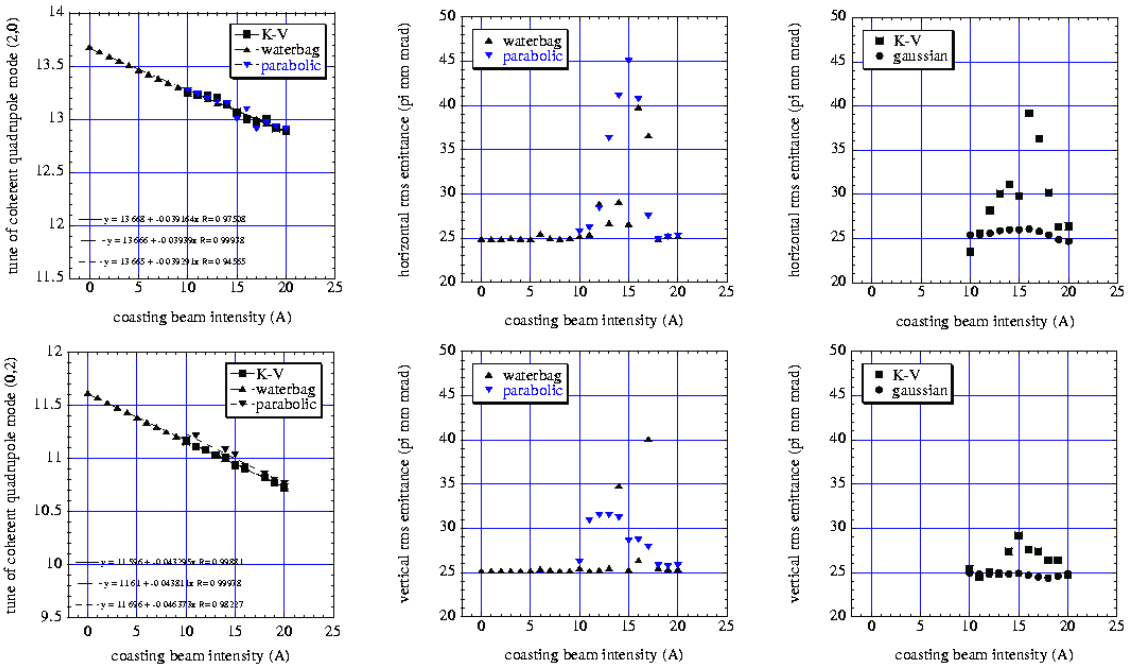

FIGURE 7. Tune of coherent quadrupole mode (left) and rms emittance at 512 turns after injection (center and right) versus beam intensity. Upper figures show horizontal results and lower ones vertical. Rms emittance growth is observed when either the horizontal or vertical coherent quadrupole tune becomes integer. (Reproduced from Ref. 9).

B Space Charge and TMCI

It was reported in a recent paper of Blaskiewicz [10] that the space-charge tune shift can strongly damp the transverse mode coupling instability (TMCI), which is also known as strong head-tail instability. The investigation was made on the basis of particle tracking and the analytically solvable *square-well air-bag model* [11], with the bunch distribution in the longitudinal phase space,

$$\Psi(\phi, \Delta E) = \tfrac{1}{2}\rho(\phi)[\delta(\Delta E - \widehat{\Delta E}) + \delta(\Delta E + \widehat{\Delta E})] \ , \qquad (3.1)$$

where $\rho(\phi) = 1/(2\pi)$ is the linear distribution or the projection onto the longitudinal axis. In this model the synchrotron phase ϕ ranges from $-\pi$ to 0 at $\Delta E = -\widehat{\Delta E}$ and from π to 0 at $\Delta E = \widehat{\Delta E}$, with $\phi = 0$ representing the head of the bunch.

What is going to be presented here is a qualitative explanation why the space charge helps TMCI. Without space charge, the bunch starts to be unstable when two neighboring synchro-betatron modes merge under the influence of the wake forces. Typically, the pure betatron mode (the azimuthal or synchrotron harmonic 0 mode, also known as the rigid-bunch mode) is affected by the wake force and

shifts downward, while the other azimuthal modes are not much affected, at least at low intensity. The transverse wake force produced by an off-axis beam has the polarity that deflects the beam further away from the pipe axis. This force acts as a defocusing force for the rigid beam mode, and therefore the frequency shifts downward. Such a down-shift of the betatron frequency is routinely observed in electron rings and serves as an important tool of probing the impedance. As a result, the instability threshold is determined by the coupling of the 0 and -1 modes, as illustrated in the left plot of Fig. 8, (see below for definitions of parameters).

The space charge by itself also shifts all the frequencies downward, as illustrated in the right plot of Fig. 8. The only exception is the azimuthal 0 mode, which describes the motion of the bunch as a whole, and, therefore, is not influenced by the space charge at all. Thus, in the presence of space charge, the 0 mode will couple with the -1 mode at a higher current intensity and therefore the threshold is raised in the presence of space charge. This is illustrated in the left plot of Fig. 9.

Let us go in more details with mathematics. The transverse displacement $x(\phi)$ of a particle at the synchrotron phase ϕ satisfies the equation of motion:

$$\frac{d^2x(\phi)}{dt^2} + \omega_\beta^2 x(\phi) = F(\phi) + S\rho(\phi)[x(\phi) - \bar{x}(\phi)] \ , \tag{3.2}$$

where $\omega_\beta/(2\pi)$ is the unperturbed betatron frequency and the smooth approximation for the betatron oscillations has been applied. To incorporate synchrotron oscillation, the full time derivative takes the form

$$\frac{d}{dt} = \frac{\partial}{\partial t} + \omega_s \frac{\partial}{\partial \phi} \ , \tag{3.3}$$

with $\omega_s/(2\pi)$ being the synchrotron frequency. The right-hand side of Eq. (3.2) contains the transverse driving forces. The first term is the transverse wake force

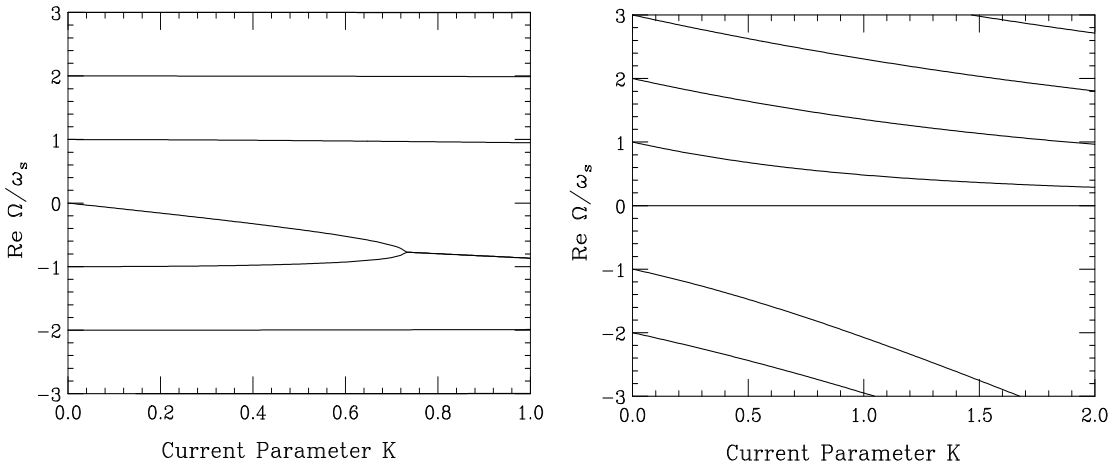

FIGURE 8. Left: The transverse wake force shifts mostly the azimuthal 0 mode downward but not the other modes. Instability occurs when the 0 and -1 modes meet with each other. Right: The space-charge force in the absence of the wake forces shifts all modes downward with the exception of the 0 mode.

$$F(\phi) = \frac{N_b e^2 c^2}{E_0 C} \int_0^{|\phi|} W_1[z(\phi') - z(\phi)]\rho(\phi')\bar{x}(\phi')d\phi' \ , \tag{3.4}$$

where N_b is the number of particles in the bunch, W_1 the transverse wake function, $z(\phi)$ the longitudinal position of the beam particle. The second term is the space-charge contribution. It is proportional to the linear density $\rho(\phi)$ and the displacement relatively the local beam center $x(\phi) - \bar{x}(\phi)$, with the constant S representing the space-charge strength.

To solve the problem quantitatively, we expand the offset into the synchrotron harmonics (or azimuthals):

$$x(\phi, t) = e^{-i\omega_\beta t - i\Omega t} \sum_{n=-\infty}^{\infty} x_n e^{in\phi} \ , \tag{3.5}$$

where $\Omega/(2\pi)$ is the collective frequency shift. In this air-bag model, all particles reside at the edge of the bunch distribution in the longitudinal phase space. Note that because of the square-well air-bag model, these synchrotron azimuthals are slightly different from the conventional ones. The average offset at the synchrotron phase ϕ is therefore given by

$$\bar{x}(\phi, t) = \tfrac{1}{2}\left[x(\phi, t) + x(-\phi, t)\right] = e^{-i\omega_\beta t - i\Omega t} \sum_{n=-\infty}^{\infty} x_n \cos n\phi \ . \tag{3.6}$$

Following basically Ref. [12], Eq. (3.2) transforms into an eigenvalue equation,

$$\left(\frac{\Omega}{\omega_s} - n\right) x_n = -K \sum_{m=-\infty}^{\infty} x_m \left(\mathcal{W}_{nm} + \xi \mathcal{Q}_{nm}\right) \ . \tag{3.7}$$

Here, the current parameter is written as

$$K = \frac{N_b e^2 c^2 W_0}{2\pi^2 \omega_\beta \omega_s C E_0} \ . \tag{3.8}$$

The wake matrix elements are then given by

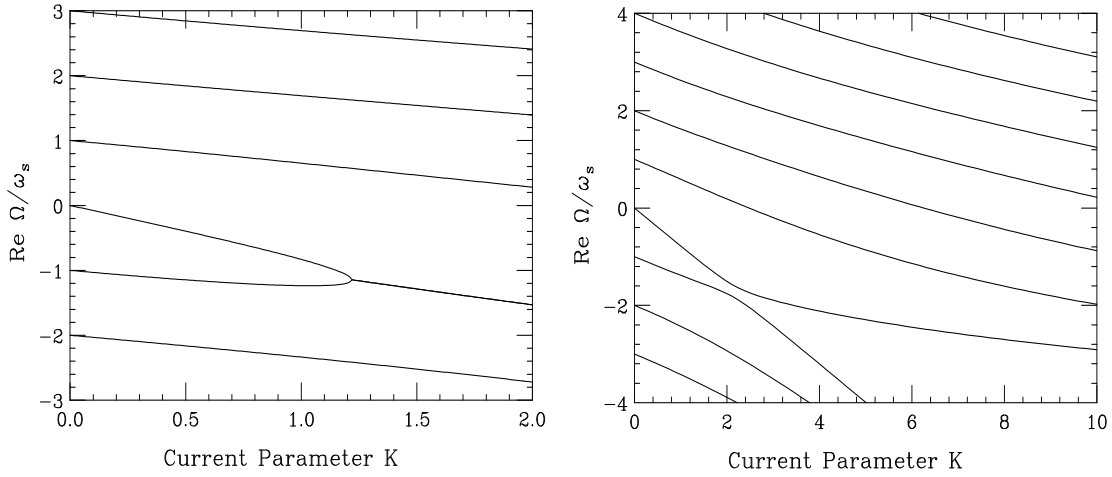

FIGURE 9. Left: With the transverse space-charge force added to the wake forces, all modes except the 0 mode are shifted downward, thus requiring the 0 and -1 modes to couple at a much higher current threshold. Right: When space charge reaches the critical value of $\xi = 5$, the -1 mode is shifted away from the 0 mode by so much that they do not couple anymore.

$$\mathcal{W}_{nm} = \int_0^{\pi} d\phi \int_0^{\phi} d\phi' w[z(\phi') - z(\phi)] \cos(n\phi) \cos(m\phi') \ , \tag{3.9}$$

where the wake function is presented as $W(z) = W_0 w(z)$ with W_0 serving as a normalizing constant. The space-charge parameter

$$\xi = \frac{\Delta\omega_\beta}{2K\omega_s} \tag{3.10}$$

is a current-dependent ratio of the incoherent tune shift

$$\Delta\omega_\beta = \frac{S\rho}{2\omega_\beta} \tag{3.11}$$

to the current parameter K. The space-charge matrix elements are

$$\mathcal{Q}_{nm} = \delta_{nm} - \delta_{n,-m} \tag{3.12}$$

in the assumed air-bag distribution.

Without wake forces, the eigenvalue equation leads to the mode behavior presented in the right plot of Fig. 8. For the simplest step-like wake function $w(z) = \theta(z)$ and without space charge ($\xi = 0$), the mode coupling is shown in the left plot of Fig. 8, where the threshold is $K = 0.73$. Now space charge is introduced with the space-charge parameter $\xi = 4$. We do see in the left plot of Fig. 9 that, because the -1 mode is shifted downward by the space charge, the instability threshold has been pushed up to $K = 1.25$ as compared with the left plot of Fig. 8.

Further increasing the space-charge parameter to $\xi = 5$, we see in the right plot of Fig. 9 that modes 0 and -1 do not merge any more. What is not shown in the plot is a much higher new threshold where the 0 mode couples with the 1 mode instead. This new threshold is very much model dependent. In the present model, it depends strongly on the number of modes included in the truncated matrix. For truncation at modes $|n| = 32$, this new threshold is at least a factor of 30 higher than when space charge is absent. A dependence of the calculated threshold K_{th} on the mode truncation number $|n|$ was found as $K_{th} \propto |n|^{1/2}$ for $|n| \leq 10$ and even weaker,

$$K_{th} \propto |n|^{1/3} \ , \tag{3.13}$$

for $10 \leq |n| \leq 32$. The divergence is caused by the fact that the Fourier components of the space charge in Eq. (3.12) do not roll off at high frequencies. Taking into account the finite value of the ratio of transverse bunch size $\sigma_\perp$ to longitudinal bunch size $\sigma_\parallel$, we estimate this roll off limit as $|n| \simeq \sigma_\perp/\sigma_\parallel \simeq 200$ to 1000 for typical hadron bunches. Extrapolation of the dependence Eq. (3.13) into this area brings to a conclusion that the actual threshold can be 2 to 3 times higher than the result reported for $|n| = 32$. So for this simplified wake-beam model, the space charge is found to be able to increase the TMCI threshold by a factor of 50 to 100.

Unlike the longitudinal mode-coupling instability where the bunch may just lengthen as the beam becomes unstable essentially without losing beam particles, this transverse instability is devastating; as soon as the threshold is reached, the bunch disappears. TMCI in electron machines are usually damped with a *reactive*

feedback system; i.e., the kicker is located at an even multiple of 90° from the pickup [13]. This implies the addition of a term $G\bar{x}(\phi)$ to the right-hand side of Eq. (3.2), where G is the gain of the feedback system. Notice that the reactive feedback acts on the center of the bunch and is *in phase* with the particle displacements; hence the term reactive. It therefore modifies the betatron tune by introducing a tune shift. Thus, only the 0 mode is affected but not the other modes. The instability threshold can then be raised by properly choosing the strength and sign of the feedback gain G so that the 0 mode has a *positive* shift. The space-charge tune shift in a proton machine, as discussed above, constitutes a natural inverse reactive feedback.

One of the authors (A. Burov) expresses his gratitude to Slava Danilov and Mike Blaskiewicz for fruitful discussions.

REFERENCES

1. J.R. Alonso, J.R., *Proceedings of the Sixth European Particle Accelerator Conference*, p.493 (Stockholm, Sweden, June 22-26, 1998).
2. *The JHF Accelerator Design Study Report*, Sept. 1997, KEK.
3. *ESS, A Next Generation Neutron Source for Europe*, Vol. 3, The ESS Technical Study, ISBN 090 237 6 500 090 237 6 659.
4. *A Development Plan for the Fermilab Proton Source*, Ed. S. Holmes, Fermilab Report TM-2021.
5. Keil, E., and Schnell, W., CERN Report TH-RF/69-48, 1969; Neil, V.K., and Sessler, A.M., *Rev. Sci. Instr.,* **36**, 429 (1965); Boussard, D., CERN Report Lab II/RF/Int./75-2, 1975.
6. Plum, M.A., Fitzgerald, D.H., Langenbrunner, J., Macek, R.J., Merrill, F.E., Neri, F, Thiessen, H.A., Walstrom, P.L., Griffin, J.E., Ng, K.Y., Qian, Z.B., Wildman, D., and Prichard, B.A. Jr., *Phys. Rev. ST Accel. Beams*, **2**, 064201 (1999).
7. Koba, K., Machida, S., and Mori, Y., KEK Note, 1997 (unpublished); Koba, K., these proceedings; Koba, K., *et al*, *Phys. Sci. Instr.*, **70**, 2988 (1999).
8. Griffin, J.E., *RF System Considerations for a Muon Collider Proton Driver Synchrotrons*, Fermilab report FN−669, 1998.
9. Machida, S., and Ikegami, M,, *Proceedings of Workshop on Space Charge Physics in High Intensity Hadron Rings*, p.73, Ed. Luccio, A.U., and Weng, W.T., (Shelter Island, New York, May 4-7, 1998).
10. Blaskiewicz, M., *Fast Head-tail Instability with Space Charge*, *Phys. Rev. ST Accel. Beams*, **1**, 044201 (1998).
11. Danilov V., and Perevedentsev, E., *Strong Head-Tail Effect and Decoupled Modes in the Space-Time Domain*, *Proceedings of XVth International Conference on High Energy Accelerators*, p.1163 (Hamburg, 1992).
12. Danilov, V., and Perevedentsev, E., *Feedback system for elimination of the TMCI*, *Nucl. Instr. and Methods*, **A391**, 77 (1997).
13. Ruth, R., CERN Report LEP-TH/83-22, 1983; Myers, S., *Proceedings of IEEE Particle Accelerator Conference*, p.503 (Washington, 1987); Zotter, B., *IEEE Trans. Nucl. Sci.*, **NS-32**, 2191 (1985); Myers, S., CERN Report LEP-523 1984.